

# Metallomics

Accepted Manuscript



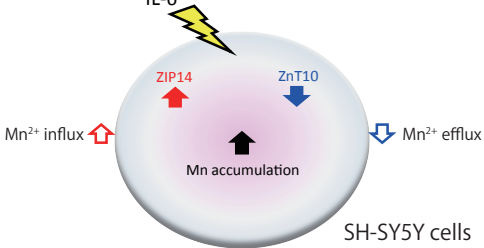
This is an *Accepted Manuscript*, which has been through the Royal Society of Chemistry peer review process and has been accepted for publication.

*Accepted Manuscripts* are published online shortly after acceptance, before technical editing, formatting and proof reading. Using this free service, authors can make their results available to the community, in citable form, before we publish the edited article. We will replace this *Accepted Manuscript* with the edited and formatted *Advance Article* as soon as it is available.

You can find more information about *Accepted Manuscripts* in the [Information for Authors](#).

Please note that technical editing may introduce minor changes to the text and/or graphics, which may alter content. The journal's standard [Terms & Conditions](#) and the [Ethical guidelines](#) still apply. In no event shall the Royal Society of Chemistry be held responsible for any errors or omissions in this *Accepted Manuscript* or any consequences arising from the use of any information it contains.

# IL-6 Metallomics



1  
2  
3  
4  
5  
6  
7  
8

1  
2  
3  
4  
5  
6  
7  
8 **Interleukin-6 enhances manganese accumulation in SH-SY5Y cells: Implications of the**  
9 **up-regulation of ZIP14 and the down-regulation of ZnT10**  
10

11  
12  
13  
14  
15  
16 **Hitomi Fujishiro, Mari Yoshida, Yuka Nakano and Seiichiro Himeno\***  
17

18  
19  
20 *Laboratory of Molecular Nutrition and Toxicology, Faculty of Pharmaceutical Sciences,*  
21 *Tokushima Bunri University, Yamashiro-cho, Tokushima, 770-8514, Japan.*

22  
23 *E-mail: himenos@ph.bunri-u.ac.jp*

24  
25 *Tel. +81-88-602-8459, Fax. +81-88-655-3051; Fax. +81-88-655-3051*  
26  
27  
28  
29  
30  
31  
32  
33  
34  
35  
36  
37  
38  
39  
40  
41  
42  
43  
44  
45  
46  
47  
48  
49  
50  
51  
52  
53  
54  
55  
56  
57  
58  
59  
60

**Abstract**

Exposure to an excess amount of manganese causes neurological symptoms similar to Parkinson's disease. Zinc transporters such as Zrt, Irt-related protein 8 (ZIP8), and ZIP14 have been shown to have affinities for  $Mn^{2+}$  as well as  $Zn^{2+}$ , but their roles in  $Mn^{2+}$  uptake in neuronal cells remain unclear. Recent studies have shown that another zinc transporter ZnT10 may be involved in manganese excretion. Here we examined the roles of ZIP8, ZIP14, and ZnT10 in the transport of manganese in human SH-SY5Y neuroblastoma cells. The introduction of siRNA of ZIP14 decreased the uptake of  $Mn^{2+}$ , suggesting a significant role of ZIP14 in  $Mn^{2+}$  uptake in SH-SY5Y cells. The pretreatment of SH-SY5Y cells with interleukin-6 (IL-6) markedly increased the accumulation of manganese to approx. 3-fold of the control, which could be partly explained by the increased uptake of  $Mn^{2+}$  due to the up-regulation of ZIP14 by IL-6. The treatment of SH-SY5Y cells with IL-6 clearly decreased both the mRNA and protein levels of ZnT10 with a concomitant decrease in the manganese excretion efficiency. These results suggest that both the up-regulation of ZIP14 and the down-regulation of ZnT10 by IL-6 might have enhanced the accumulation of manganese in SH-SY5Y cells. Our results provide new insight into the roles of zinc transporters in the aberrant manganese accumulation in neuronal cells, particularly in the presence of inflammatory cytokines such as IL-6.

**Keywords:** manganese, zinc transporter, ZnT10, ZIP14, interleukin-6, Parkinsonism

## Introduction

Manganese is an essential element that functions as a co-factor for many enzymes such as superoxide dismutase, arginase, glycosyltransferases, and glutamine synthetase.<sup>1,2</sup> Occupational exposure to manganese causes neurological symptoms called manganism which resembles the symptoms of Parkinson's disease (PD).<sup>3</sup> The mechanisms of manganese transport in the nervous system are not well understood.

Earlier studies have presumed that the major mediator of manganese incorporation into the brain is transferrin, which can bind  $Mn^{3+}$  and is incorporated into cells via endocytosis after binding to transferrin receptor.<sup>4</sup> However, speciation analyses of chemical forms of manganese have revealed that not only transferrin-bound  $Mn^{3+}$  but low-molecular-weight  $Mn^{2+}$ -containing substances are also detected in human blood serum and cerebrospinal fluid, suggesting that both  $Mn^{3+}$  and  $Mn^{2+}$  play important roles in neuronal manganese accumulation.<sup>5,6</sup> A well-known transporter with affinity for  $Mn^{2+}$  is divalent metal transporter 1 (DMT1), and its role in the transport of  $Mn^{2+}$  has been studied in neuronal cells.<sup>7</sup> However, the incorporation of  $Mn^{2+}$  into neuronal cells cannot be explained solely by the functioning of DMT1,<sup>8,9</sup> suggesting that other metal transporters may participate in  $Mn^{2+}$  transport in neuronal cells.

Zinc transporters have also been shown to be involved in the cellular transport of manganese. Mammalian zinc transporters consists of two families: 14 members of the ZIP family encoded by *SLC39A* genes, which play a role in increasing cytosolic zinc, and 10 members of the ZnT family encoded by *SLC30A* genes, which play a role in decreasing cytosolic zinc.<sup>10</sup> Among the ZIP family transporters, ZIP8 and ZIP14 have affinities to  $Mn^{2+}$  and  $Cd^{2+}$  in addition to  $Zn^{2+}$ .<sup>11-13</sup> In previous studies, we demonstrated that the down-regulation of ZIP8 resulted in decreases in the uptake of  $Mn^{2+}$  and  $Cd^{2+}$  into cells, by using siRNA transfection and by developing Mn-resistant cell lines.<sup>14-17</sup> However, it remains

1  
2  
3 unknown whether ZIP8 and ZIP14 are actually involved in the transport of  $Mn^{2+}$  in the  
4 nervous system.  
5  
6

7  
8 In addition to ZIP8 and ZIP14, recent studies have shown that another zinc transporter,  
9 ZnT10 encoded by *SLC30A10*, plays a pivotal role in the transport of manganese in the  
10 human brain. Two studies reported that the mutations in *SLC30A10* gene in humans resulted  
11 in both the hyperaccumulation of manganese in the brain and neurological disorders including  
12 Parkinsonism, and the authors of those studies suggested that ZnT10 is involved in the efflux  
13 of cellular manganese.<sup>18,19</sup>  
14  
15  
16  
17  
18  
19

20  
21 Extensive evidence has demonstrated that inflammatory cytokines such as IL-1 $\beta$ , tumor  
22 necrosis factor- $\alpha$  (TNF- $\alpha$ ), and IL-6 are deeply associated with the pathogenesis of PD and  
23 other neurodegenerative disorders.<sup>20</sup> In PD patients, activated microglia, which produce  
24 inflammatory cytokines, were detected in the brain, and elevated levels of IL-6 and other  
25 cytokines have been found in blood serum and cerebrospinal fluid.<sup>21</sup> Among the ZIP family  
26 transporters, ZIP14 has a unique feature relevant to IL-6; the expression of ZIP14 in the liver  
27 of mice was shown to be induced by IL-6, leading to enhanced hepatic zinc accumulation and  
28 resultant hypozincemia.<sup>22</sup> To our knowledge, however, no study has investigated the effects of  
29 IL-6 on the expression of ZIP14 in neuronal cells and on the transport of  $Mn^{2+}$ .  
30  
31  
32  
33  
34  
35  
36  
37  
38  
39

40  
41 In the present study, we examined the roles of DMT1, ZIP8, and ZIP14 in the uptake of  
42  $Mn^{2+}$  by using siRNA transfection in human neuroblastoma SH-SY5Y cells. We also  
43 examined the effects of IL-6 on the expressions of DMT1, ZIP8, ZIP14, and ZnT10, and on  
44 the transport of manganese. We show here that treatment of SH-SY5Y cells with IL-6  
45 markedly enhanced manganese accumulation, probably due to both the up-regulation of ZIP8  
46 and ZIP14 and the down-regulation of ZnT10.  
47  
48  
49  
50  
51  
52  
53  
54  
55  
56  
57  
58  
59  
60

## Experimental

### Materials

[<sup>54</sup>Mn]-MnCl<sub>2</sub> was purchased from PerkinElmer (Boston, MA, USA). [<sup>109</sup>Cd]-CdCl<sub>2</sub> and [<sup>65</sup>Zn]-ZnCl<sub>2</sub> were purchased from RIKEN (Saitama, Japan). Human recombinant IL-6 was purchased from R&D Systems (Minneapolis, MN). Rabbit anti-β-actin polyclonal antibody and anti-rabbit IgG, HRP-linked antibody were purchased from Cell Signaling Technology (Danvers, MA). Rabbit anti-Nramp2 (DMT1) polyclonal antibody was purchased from Santa Cruz Biotechnology (Santa Cruz, CA). Rabbit anti-ZIP8 polyclonal antibody was purchased from Proteintech (Chicago, IL). Rabbit anti-ZnT10 polyclonal antibody was purchased from Abcam (Cambridge, MA). Rabbit anti-ZIP14 polyclonal antibody was produced by Operon Biotechnologies (Tokyo, Japan).

### Cell culture

Human SH-SY5Y neuroblastoma cells (A.T.C.C., Manassas, VA) were cultured in Dulbecco's modified Eagle's medium (DMEM)/F12 medium supplemented with 10% fetal bovine serum (FBS) and penicillin and streptomycin under 5% CO<sub>2</sub> at 37°C.

### Semi-quantitative RT-PCR and real-time RT-PCR

Total RNA was extracted and purified from cells using an SV Total RNA Isolation System (Promega, Madison, WI). The reverse transcription (RT) reaction was performed as described.<sup>16</sup> The amplification profile for ZIP8, ZIP14, DMT1 and β-actin consisted of an initial denaturation at 94°C for 5 min, then 28-45 cycles of denaturation at 94°C for 30 sec, annealing at 55-57°C for 30 sec, and extension at 72°C for 1 min. An automated DNA thermal cycler (Takara Bio Inc., Shiga, Japan) was used.

The following oligonucleotides were used for RT-PCR: as ZIP8 primers of 5' sense and 3'

1  
2  
3 antisense, 5'- CTTATTCCAGAGGCATTTGGA -3' and 5'-  
4 TCTGACAGTTTGGGCCCTTCA -3'; as ZIP14 primers of 5' sense and 3' antisense, 5'-  
5 TCCAAGAAGGACCAGGAGGAG -3' and 5'- AATATACAAGAACATTCCTCCAGC -3';  
6  
7 as DMT1 primers of 5' sense and 3' antisense, 5'- TTGGACAAATATGGCTTGCGGAAGC  
8 -3' and 5'- GCACAACACCCCCTTTGTAGATGT -3'; and as  $\beta$ -actin primers of 5' sense and  
9 3' antisense; 5'- GACCTGGCTGGCCGGGACCTG -3' and 5'-  
10 CACATCTGCTGGAAGGTGGA -3', respectively. PCR fragments were analyzed by  
11 electrophoresis on a 1.5% agarose gel.  
12  
13  
14  
15  
16  
17  
18  
19

20  
21 In the case of ZnT10, real-time RT-PCR was performed in a StepOnePlus real time PCR  
22 system (Applied Biosystems, Alameda, CA). The reaction mixture contained 10  $\mu$ L of 2 $\times$   
23 SYBR Premix Ex Taq<sup>TM</sup> (Takara Bio), 0.4  $\mu$ L of 50  $\times$  ROX Reference Dye, 0.4  $\mu$ L of 10  $\mu$ M  
24 forward and reverse primer mix, and 2  $\mu$ L of RT product. The reaction mixture was initially  
25 heated at 95°C for 5 min and then subjected to 40 thermal cycles (95°C for 5 sec and 60°C for  
26  
27 forward and reverse primer mix, and 2  $\mu$ L of RT product. The reaction mixture was initially  
28 heated at 95°C for 5 min and then subjected to 40 thermal cycles (95°C for 5 sec and 60°C for  
29  
30 1 min). PCR primers for ZnT10 and  $\beta$ -actin were purchased from BioNEER (Alameda, CA).  
31  
32  
33  
34  
35

### 36 **Measurement of metal concentrations in cells**

37  
38 We measured the manganese concentrations in cells using tracers of <sup>54</sup>Mn as described.<sup>16</sup>  
39 SH-SY5Y cells (3  $\times$  10<sup>5</sup> cells in 6-well dishes) were cultured for 24 h, pre-incubated with  
40 FBS-free media for 30 min, and then exposed to MnCl<sub>2</sub>. For the measurement of the 24-h  
41 accumulation of manganese, cells were exposed to 1  $\mu$ M [<sup>54</sup>Mn]-labeled MnCl<sub>2</sub> for 24 h in  
42 FBS-containing media. Since the cellular concentrations of manganese increase linearly up to  
43 1 h, the cellular concentrations of manganese at 1 h after the addition of 1  $\mu$ M [<sup>54</sup>Mn]-labeled  
44 MnCl<sub>2</sub> in FBS-free media were determined as the indicator of the initial uptake rate of Mn<sup>2+</sup>.  
45  
46  
47  
48  
49  
50  
51  
52

53 After the exposure to Mn<sup>2+</sup> for 1 h or 24 h, the cells were washed three times with 0.5 mL  
54 ice-cold medium containing FBS followed by a wash with phosphate buffered saline (PBS)  
55 containing 0.05% EDTA, and then harvested with 1.0 mL PBS containing 0.5% trypsin/EDTA  
56  
57  
58  
59  
60

1  
2  
3 and transferred to a test tube. For the measurement of the cells' efficiency of manganese  
4 excretion, SH-SY5Y cells were cultured for 24 h, treated with 1  $\mu\text{M}$  [ $^{54}\text{Mn}$ ]-labeled  $\text{MnCl}_2$  for  
5 8 h, and then washed with 0.5 mL of PBS containing 0.05% EDTA three times. After the  
6 medium was changed to a  $\text{MnCl}_2$ -free medium, the cells were further incubated for 30 and 60  
7 min, and then harvested as described above. In the experiment with IL-6, cells were pretreated  
8 with IL-6 (100 ng/mL) for 24 h and then exposed to  $\text{MnCl}_2$  after the change of the media. The  
9 radioactivity of  $^{54}\text{Mn}$  was measured using an auto-well gamma counter (ARC-300; Aloka,  
10 Tokyo). All experiments were carried out three times and the average values were used.  
11  
12  
13  
14  
15  
16  
17  
18  
19  
20  
21  
22

### 23 **Knockdown of DMT1, ZIP8, and ZIP14 in SH-SY5Y cells**

24 The siRNAs targeting DMT1, ZIP8, and ZIP14 (Custom siSET-3, SYD21-325) were  
25 purchased from B-Bridge International (Cupertino, CA). The control siRNA consists of 20-25  
26 nucleotides with a scrambled sequence. Transfection of siRNA was performed by using a  
27 SH-SY5Y cell Nucleofector kit V (Lonza, Gaithersburg, MD) according to the manufacture's  
28 protocol. SH-SY5Y cells ( $1 \times 10^6$  cells) were incubated with Nucleofector V solution and  
29 transfected with each of 100 nM siRNAs. Cells were incubated for 48 h after the transfection  
30 and then used for the assays of manganese accumulation.  
31  
32  
33  
34  
35  
36  
37  
38  
39  
40  
41  
42

### 43 **Western blot analysis**

44 Proteins were separated by 10% SDS polyacrylamide gel electrophoresis and  
45 electrophoretically transferred to a polyvinylidene fluoride membrane. The transblot was  
46 preincubated with 5% non-fat dry skim milk in Tris-buffered saline (TBS) pH 7.4, and then  
47 incubated with anti-ZIP8, anti-ZIP14, anti-DMT1, and anti- $\beta$ -actin antibody overnight. The  
48 membrane was washed with TBS/0.05% Tween 20 and then incubated with anti-rabbit IgG,  
49 HRP-linked antibody (1:3000). After the membrane was washed with TBS/0.05% Tween 20,  
50 immunoreactive bands were detected using enhanced chemiluminescence reagents. When  
51  
52  
53  
54  
55  
56  
57  
58  
59  
60

1  
2  
3 immunoblotting was performed using goat anti-rabbit IgG antibody, the membrane was  
4 treated as recommended by the manufacturer. In addition to SH-SY5Y cells, human cell lines  
5  
6 including HepG2 hepatocellular carcinoma cells, hFOB1.19 osteoblast cells, HK-2 renal  
7 proximal tubular cells, PC3 prostate carcinoma cells, and DLD-1 colorectal adenocarcinoma  
8 cells (A.T.C.C.) were used for western blot analyses of ZIP8 and ZIP14.  
9

### 10 11 12 13 14 15 16 17 **Statistics**

18 Data are expressed as mean  $\pm$  S.D. Significant differences were determined by Student's  
19 *t*-test.  
20  
21  
22  
23  
24  
25  
26  
27  
28  
29  
30  
31  
32  
33  
34  
35  
36  
37  
38  
39  
40  
41  
42  
43  
44  
45  
46  
47  
48  
49  
50  
51  
52  
53  
54  
55  
56  
57  
58  
59  
60

## Results

### Roles of DMT1, ZIP8, and ZIP14 in manganese uptake in SH-SY5Y cells

Figure 1A-C shows the expression profiles of ZIP8, ZIP14, and DMT1 in SH-SY5Y cells transfected with either control (scrambled sequence) or target siRNAs as measured by semi-quantitative RT-PCR and western blot analysis. The results of the control siRNA groups confirmed the expression of DMT1, ZIP8, and ZIP14 in SH-SY5Y cells under basal conditions. Figure 1D-F shows the uptake of  $Mn^{2+}$  during the initial 1 h in siRNA-transfected cells. As the control cells showed a variation in  $Mn^{2+}$  uptake, the comparison was made between the paired cells simultaneously treated with the siRNAs of control and each metal transporter. As expected, the transfection of DMT1 siRNA reduced the uptake of  $Mn^{2+}$  to about 50% of that in control cells (Fig. 1D). The transfection of ZIP8 siRNA did not alter the uptake of  $Mn^{2+}$  (Fig. 1E), while the transfection of ZIP14 siRNA decreased the uptake of  $Mn^{2+}$  to about 40% of the control (Fig. 1F). These data suggest that ZIP14, in addition to DMT1, plays an important role in the uptake of  $Mn^{2+}$  in SH-SY5Y cells. The lack of the effect of ZIP8 siRNA transfection on  $Mn^{2+}$  uptake prompted us to examine the basal expression level of ZIP8 in SH-SY5Y cells. The expression profiles of ZIP8 and ZIP14 among six types of human cell lines were examined by western blot analysis (Fig. 2). As expected, high amounts of ZIP8 and ZIP14 proteins were found in cell lines derived from liver (HepG2) and kidney (HK-2). The protein level of ZIP14 in SH-SY5Y cells was approximately similar to those in HepG2 and HK-2, whereas only a faint amount of ZIP8 protein was detected in SH-SY5Y cells when the band intensities were adjusted to that of HK-2 cells. These data suggest negligible roles of ZIP8 in SH-SY5Y cells under physiological conditions, and may explain the lack of the effects of ZIP8 siRNA transfection on  $Mn^{2+}$  uptake.

### Effects of IL-6 on metal transporter expression and manganese accumulation in

### SH-SY5Y cells

We next examined whether treatment with IL-6 enhances the expressions of ZIP8, ZIP14, and DMT1 in SH-SY5Y cells. As shown in Fig. 3, the mRNA levels of ZIP14 were increased at 3 and 12 h after the addition of IL-6 in the media. A clear increase in the protein level of ZIP14 was detected at 24 h. Treatment with IL-6 also induced the expression of ZIP8 at both the mRNA and protein levels. In contrast, there were no discernible changes in the mRNA or protein levels of DMT1 after treatment with IL-6.

We investigated whether the accumulation of manganese in SH-SY5Y cells is enhanced by pretreatment with IL-6 for 24 h. As shown in Fig. 4A, manganese accumulation was increased by IL-6 to almost 3-fold that of the control cells. To examine whether the increased accumulation of manganese is caused by the increased initial uptake of  $Mn^{2+}$ , we determined the effect of IL-6 on the 1-h uptake of  $Mn^{2+}$ . IL-6 treatment resulted in a modest but significant increase in the uptake of  $Mn^{2+}$  (Fig. 4B), suggesting that the enhanced expression of ZIP14 may be involved at least partly in the increased accumulation of manganese in SH-SY5Y cells treated with IL-6.

We next examined the expression levels of ZnT10 in SH-SY5Y cells treated with IL-6. The treatment with IL-6 resulted in decreases in the mRNA levels of ZnT10 to approx. 50% at 3 and 12 h (Fig. 5A). The protein level of ZnT10 was markedly decreased at 24 h after IL-6 treatment (Fig. 5B). To examine whether the IL-6-induced decrease in ZnT10 expression affects the excretion of manganese, we determined the manganese excretion efficiency in SH-SY5Y cells which were treated with IL-6 for 24 h, incubated with  $Mn^{2+}$  for 8 h, and then incubated further with  $Mn^{2+}$ -free media. IL-6 treatment significantly suppressed the excretion of manganese from SH-SY5Y cells (Fig. 5C).

These results suggest that the marked increase in manganese accumulation in SH-SY5Y cells treated with IL-6 was caused by the sum of the increased uptake and decreased excretion of manganese, which are associated with the IL-6-induced up-regulation of ZIP14 and ZIP8

1  
2  
3 and the down-regulation of ZnT10, respectively.  
4  
5  
6

## 7 8 **Discussion** 9

10  
11 Here we investigated whether ZIP8 and ZIP14 have any roles in  $Mn^{2+}$  uptake in  
12 neuroblastoma SH-SY5Y cells, and whether the treatment of these cells with IL-6 affects the  
13 expression of zinc transporters and alters the transport of manganese. The results obtained by  
14 siRNA transfection showed that ZIP14, in addition to DMT1, may play an important role in  
15  $Mn^{2+}$  uptake in SH-SY5Y cells (Fig. 1). IL-6 treatment markedly enhanced the 24-h  
16 accumulation of manganese (Fig. 4A) concomitant with an increase in the uptake (Fig. 4B)  
17 and a decrease in the excretion (Fig. 5C) of manganese. These changes in manganese  
18 transport might have been caused by the up-regulation of ZIP14 (Fig. 3) as well as the  
19 down-regulation of ZnT10 (Fig. 5). Since IL-6 plays important roles in the pathogenesis of  
20 PD and other neurodegenerative disorders, our results have provided new insight into the  
21 roles of ZIP14 and ZnT10, and their regulation by IL-6 in the development of manganese as  
22 well as idiopathic PD.  
23  
24  
25  
26  
27  
28  
29  
30  
31  
32  
33  
34  
35  
36  
37

38 The cellular transport of manganese has been shown to be shared with a variety of  
39 transport systems responsible for iron, calcium, and zinc. The transferrin/transferrin receptor  
40 system and DMT1 are postulated to play roles in the uptake of  $Mn^{3+}$  and  $Mn^{2+}$ , respectively.<sup>4,7</sup>  
41 Some types of calcium ATPase have an affinity for  $Mn^{2+}$  as well.<sup>23</sup> Among the zinc  
42 transporters, ZIP8 and ZIP14 have affinities not only for  $Zn^{2+}$  but also for  $Mn^{2+}$  and  $Cd^{2+}$ .<sup>11,12</sup>  
43 Although the roles of ZIP8 and ZIP14 in the uptake of  $Cd^{2+}$  have been extensively  
44 studied,<sup>14-17</sup> the roles of these zinc transporters in  $Mn^{2+}$  uptake in the neuronal cells are not yet  
45 fully understood. In the present study, we showed that the knockdown of ZIP14 by siRNA  
46 transfection reduced the uptake of  $Mn^{2+}$  into SH-SY5Y cells to about 40% of the control even  
47 in the presence of DMT1, suggesting that ZIP14 may also play a significant role in the uptake  
48  
49  
50  
51  
52  
53  
54  
55  
56  
57  
58  
59  
60

1  
2  
3 of  $Mn^{2+}$ , which could not be completely compensated for by DMT1.  
4

5  
6 The unique feature of ZIP14 as a transporter inducible by IL-6, which was first  
7 recognized in the liver,<sup>22</sup> was also observed here in neuronal SH-SY5Y cells. In addition to  
8 ZIP14, we found that IL-6 treatment also enhanced the expression of ZIP8 (Fig. 3). In accord  
9 with our results, the induction of ZIP8 expression by TNF- $\alpha$  through the transactivation of  
10 NF- $\kappa$ B has been reported in human lung cell lines.<sup>24</sup> Since the sequences indicative of Nf- $\kappa$ B,  
11 STAT, and C/EBP $\beta$  binding sites are found in the promoter regions of human ZIP8 and ZIP14,  
12 it is predictable that both ZIP8 and ZIP14 are inducible by IL-6. However, the siRNA  
13 transfection experiment suggested a minimal role of ZIP8 in SH-SY5Y cells (Fig. 1).  
14 Furthermore, the basal level of ZIP8 was very low in SH-SY5Y cells compared with other  
15 human cell lines (Fig. 2). It seems likely that physiological role of ZIP8 at its basal expression  
16 level in the uptake of  $Mn^{2+}$  in SH-SY5Y cells may be minimal and could be readily  
17 compensated by DMT1 and ZIP14 when the expression of ZIP8 was down-regulated (Fig.  
18 1E). Although the roles of both ZIP8 and ZIP14 in the enhanced uptake of  $Mn^{2+}$  have already  
19 been demonstrated in ZIP8- or ZIP14-overexpressed mouse fibroblast cells.<sup>11, 12</sup>, the enhanced  
20 uptake of  $Mn^{2+}$  observed in SH-SY5Y cells treated with IL-6 (Fig. 4B) may be caused  
21 primarily by the induction of ZIP14. Further studies are required to elucidate the roles of ZIP8  
22 in  $Mn^{2+}$  uptake in neuronal cells.  
23  
24  
25  
26  
27  
28  
29  
30  
31  
32  
33  
34  
35  
36  
37  
38  
39  
40  
41

42 The most striking finding in this study is the down-regulation of ZnT10 by IL-6 treatment.  
43 The mutations in *SLC30A10* gene encoding ZnT10 were shown to cause the  
44 hyperaccumulation of manganese in the brain and neurological disorders similar to PD.<sup>18-19</sup> It  
45 is suggested that ZnT10 is involved in the excretion of manganese from cells, though the  
46 mechanism remains unknown.<sup>18,19</sup> ZnT10 has similarity in its amino acid sequence to ZnT1,  
47 which is responsible for the efflux of  $Zn^{2+}$  from the cytosol to the extracellular space, and it  
48 has a unique motif of NxxD similar to the other transporters related to manganese transport.<sup>19</sup>  
49 Although these genetic studies have revealed the important role of ZnT10 in manganese  
50  
51  
52  
53  
54  
55  
56  
57  
58  
59  
60

1  
2  
3 transport, endogenous or environmental factors affecting the expression and functions of  
4 ZnT10 remain unknown.  
5  
6

7  
8 Our study demonstrated for the first time that IL-6 can down-regulate the expression of  
9 ZnT10, leading to a decrease in manganese excretion in neuronal cells. As both the mRNA  
10 and protein levels of ZnT10 were decreased by IL-6 treatment (Fig. 5), IL-6 might have  
11 affected the transcription of *SCL30A10* gene. Compared with the up-regulation of ZIP8 and  
12 ZIP14 by IL-6, completely different mechanisms may participate in the down-regulation of  
13 ZnT10 by IL-6. A recent report on ZnT10 expression has suggested a possible involvement of  
14 a regulation element,<sup>25</sup> but further studies are required to elucidate the precise mechanism of  
15 how IL-6 down-regulates the transcription of *SLC30A10* gene.  
16  
17  
18  
19  
20  
21  
22  
23  
24

25 It should be noted here that manganese exposure itself can enhance the production of  
26 IL-6 in microglia of the brain<sup>26</sup> and in the liver.<sup>27</sup> In the development of manganese due to  
27 exposure to manganese, the activation of IL-6 production by manganese may further  
28 exacerbate the neuronal manganese accumulation by the alterations in the expression of zinc  
29 transporters. Further, as many types of neurodegenerative disorders including PD and  
30 Alzheimer's disease are associated with the enhancement of cytokine production in the  
31 brain,<sup>20</sup> more attention should be paid to the roles of IL-6 and other cytokines in the lowered  
32 expression of ZnT10 in Alzheimer's disease<sup>28</sup> and in the aberrant manganese accumulation in  
33 idiopathic PD patients.<sup>29</sup>  
34  
35  
36  
37  
38  
39  
40  
41  
42  
43  
44  
45  
46

## 47 **Conclusion**

48  
49  
50 The present findings provide evidence that IL-6 can modify the expression of zinc  
51 transporters such as ZIP8, ZIP14, and ZnT10 that are involved in manganese transport.  
52  
53 Although other transport systems are also involved in the transport of manganese under  
54 normal conditions, these zinc transporters may play greater roles in the dysregulation of metal  
55  
56  
57  
58  
59  
60

1  
2  
3 homeostasis when inflammatory events are activated by neurodegenerative disorders. Further  
4  
5 mechanistic studies will elucidate the roles of zinc transporters in the pathophysiology of  
6  
7 neurodegenerative disorders including PD.  
8  
9

### 10 11 12 13 14 **Acknowledgements**

15  
16  
17  
18 This work was partly supported by a JSPS KAKENHI Grant-in-Aid for Scientific Research  
19  
20 (B-22390127 to SH and C-24590168 to HF).  
21  
22  
23  
24  
25  
26  
27  
28  
29  
30  
31  
32  
33  
34  
35  
36  
37  
38  
39  
40  
41  
42  
43  
44  
45  
46  
47  
48  
49  
50  
51  
52  
53  
54  
55  
56  
57  
58  
59  
60

## Figure legends

**Fig. 1** Effects of knockdown of DMT1, ZIP8 or ZIP14 expression by siRNA transfection on the uptake of  $Mn^{2+}$  in SH-SY5Y cells. Semi-quantitative RT-PCR and western blot analysis of DMT1 (A), ZIP8 (B), and ZIP14 (C) were carried out 48 h after the transfection of siRNA for control (scrambled sequence) or each metal transporter. The numbers on the western blot show the relative intensity of the bands determined by densitometry. The effects of transfection of siRNAs of DMT1 (D), ZIP8 (E), or ZIP14 (F) on the uptake of  $1 \mu M Mn^{2+}$  for 1 h were examined in SH-SY5Y cells. The experiments were repeated three to five times. Significantly different from control siRNA-transfected cells,  $**p < 0.01$ .

**Fig. 2** Protein levels of ZIP8 and ZIP14 were compared among six types of human cell lines by western blot analysis. SH-SY5Y, neuroblastoma cells; HepG2, hepatocellular carcinoma cells; hFOB, hFOB1.19 osteoblast cells; HK-2, renal proximal tubular cells; PC3, prostate carcinoma cells; DLD-1, colorectal adenocarcinoma cells.  $\beta$ -actin was used as a loading control.

**Fig. 3** Treatment of SH-SY5Y cells with IL-6 resulted in the up-regulation of ZIP8 and ZIP14, but not DMT1. SH-SY5Y cells were incubated with IL-6 (100 ng/mL) for different time intervals, and the levels of mRNA and protein of each metal transporter were determined by semi-quantitative RT-PCR (A) and western blot analysis (B).  $\beta$ -actin was used as a loading control. The reproducibility of PCR and western blotting was confirmed by repeated (3-5 times) experiments.

**Fig. 4** Effects of IL-6 on 24-h accumulation and 1-h uptake of  $Mn^{2+}$  in SH-SY5Y cells. Cells were stimulated with IL-6 (100 ng/ml) for 24 h and exposed to [ $^{54}Mn$ ]-labeled  $MnCl_2$  ( $1 \mu M$ )

1  
2  
3 for 24 h (A) or 1 h (B) for the measurement of accumulation and uptake of  $Mn^{2+}$ , respectively.  
4  
5 The experiments were repeated three to five times. Data are means  $\pm$  SD of triplicate  
6  
7 experiments. Significantly different from untreated cells, \* $p < 0.05$ .  
8  
9

10  
11 **Fig. 5** Effects of IL-6 on the expression of ZnT10 and the manganese excretion efficiency in  
12 SH-SY5Y cells. Cells were incubated with IL-6 for 0, 3, 12, and 24 h, and the levels of  
13 mRNA and protein were determined by real time RT-PCR (A) and western blot analysis (B).  
14  
15 The manganese excretion efficiency was determined in SH-SY5Y cells pretreated with IL-6  
16 for 24 h, exposed to  $MnCl_2$  (1  $\mu M$ ) for 8 h, and then incubated further with  $Mn^{2+}$ -free medium.  
17  
18 The concentrations of manganese retained in cells were determined at 0, 30 and 60 min after  
19 the medium was changed. The experiments were repeated three to five times. Data are means  
20  
21  $\pm$  SD of triplicate experiments. Significantly different from untreated cells, \* $p < 0.05$ .  
22  
23  
24  
25  
26  
27  
28  
29  
30  
31  
32  
33  
34  
35  
36  
37  
38  
39  
40  
41  
42  
43  
44  
45  
46  
47  
48  
49  
50  
51  
52  
53  
54  
55  
56  
57  
58  
59  
60

## References

- 1 C. L. Keen, J. L. Ensunsa, M. S. Clegg, *Met. Ions Biol. Syst.*, 2000, **37**, 89-121.
- 2 L.S. Hurley, C. L. Keen, *Manganese*. In: Underwood E, Mertz W, editors. Academic Press; New York, 1987, 185-225.
- 3 A. Barbeau, N. Inoue, T. Cloutier, *Adv. Neurol.*, 1976, **14**, 339-352.
- 4 R. C. Keefer, A. J. Barak, J. D. Boyett, *Biochim. Biophys. Acta.*, 1970, **221**, 390-393.
- 5 B. Michalke, A. Berthele, P. Mistriotis, M. Ochsenkuhn-Petropoulou, S. Halbach, *J. Trace Elem. Med. Biol.*, 2007, **21** Suppl 1, 4-9.
- 6 R. A. Yokel, *Neuromolecular Med.*, 2009, **11**, 297-310.
- 7 J. A. Roth, S. Singleton, J. Feng, M. Garrick, P. N. Paradkar, *J. Neurochem.*, 2010, **113**, 454-464.
- 8 J. S. Crossgrove, R. A. Yokel, *Neurotoxicology*, 2004, **25**, 451-460.
- 9 A. C. Chua, E. H. Morgan, *Biol. Trace Elem. Res.*, 1996, **55**, 39-54.
- 10 T. Fukada, T. Kambe, *Metallomics*, 2011, **3**, 662-674.
- 11 L. He, K. Girijashanker, T. P. Dalton, J. Reed, H. Li, M. Soleimani, D. W. Nebert, *Mol. Pharmacol.*, 2006, **70**, 171-180.
- 12 K. Girijashanker, L. He, M. Soleimani, J. M. Reed, H. Li, Z. Liu, B. Wang, T. P. Dalton, D. W. Nebert, *Mol. Pharmacol.*, 2008, **73**, 1413-1423.
- 13 S. Himeno, T. Yanagiya, H. Fujishiro, *Biochimie*, 2009, **91**, 1218-1222.
- 14 H. Fujishiro, S. Okugaki, K. Kubota, T. Fujiyama, H. Miyataka, S. Himeno, *J. Appl. Toxicol.*, 2009, **29**, 367-373.
- 15 H. Fujishiro, M. Doi, S. Enomoto, S. Himeno, *Metallomics*, 2011, **3**, 710-718.
- 16 H. Fujishiro, T. Ohashi, M. Takuma, S. Himeno, *Metallomics*, 2013, **5**, 437-444.
- 17 H. Fujishiro, Y. Yano, Y. Takada, M. Tanihara, S. Himeno, *Metallomics*, 2012, **4**, 700-708.
- 18 M. Quadri, A. Federico, T. Zhao, G. J. Breedveld, C. Battisti, C. Delnooz, L. A. Severijnen, L. Di Toro Mammarella, A. Mignarri, L. Monti, A. Sanna, P. Lu, F. Punzo, G. Cossu, R. Willemsen, F. Rasi, B. A. Oostra, B. P. van de Warrenburg, V. Bonifati, *Am. J. Hum. Genet.*, 2012, **90**, 467-477.
- 19 K. Tuschl, P. T. Clayton, S.M. Gospe, Jr., S. Gulab, S. Ibrahim, P. Singhi, R. Aulakh, R. T. Ribeiro, O. G. Barsottini, M. S. Zaki, M. L. Del Rosario, S. Dyack, V. Price, A. Rideout, K. Gordon, R. A. Wevers, W. K. Chong, P. B. Mills, *Am. J. Hum. Genet.*, 2012, **90**, 457-466.
- 20 L. M. Collins, A. Toulouse, T. J. Connor, Y. M. Nolan, *Neuropharmacology*, 2012, **62**, 2154-2168.
- 21 D. Blum-Degen, T. Muller, W. Kuhn, M. Gerlach, H. Przuntek, P. Riederer, *Neurosci. Lett.*, 1995, **202**, 17-20.
- 22 J. P. Liuzzi, L. A. Lichten, S. Rivera, R. K. Blanchard, T. B. Aydemir, M. D. Knutson, T. Ganz, R. J. Cousins, *Proc. Natl. Acad. Sci. U S A*, 2005, **102**, 6843-6848.

- 1  
2  
3 23 V. K. Ton, D. Mandal, C. Vahadji, R. Rao, *J. Biol. Chem.*, 2002, **277**, 6422-6427.  
4  
5 24 J. R. Napolitano, M. J. Liu, S. Bao, M. Crawford, P. Nana-Sinkam, E. Cornet-Boyaka, D.  
6 L. Knoell, *Am. J. Physiol. Lung Cell Mol. Physiol.*, 2012, **302**, L909-918.  
7  
8 25 L. J. Coneyworth, K. A. Jackson, J. Tyson, H. J. Bosomworth, E. van der Hagen, G. M.  
9 Hann, O. A. Ogo, D. C. Swann, J. C. Mathers, R. A. Valentine, D. Ford, *J. Biol. Chem.*,  
10 2012, **287**, 36567-36581.  
11  
12 26 P. L. Crittenden, N. M. Filipov, *Toxicol. In Vitro*, 2008, **22**, 18-27.  
13  
14 27 K. Kobayashi, J. Kuroda, N. Shibata, T. Hasegawa, Y. Seko, M. Satoh, C. Tohyama, H.  
15 Takano, N. Imura, K. Sakabe, H. Fujishiro, S. Himeno, *J. Pharmacol. Exp. Ther.*, 2007,  
16 **320**, 721-727.  
17  
18 28 H. J. Bosomworth, P. A. Adlard, D. Ford, R. A. Valentine, *PLoS One*, 2013, **8**, e65475.  
19  
20 29 T. Fukushima, X. Luo, H. Kanda, *Neuroepidemiology*, 2010, **34**, 18-24.  
21  
22  
23  
24  
25  
26  
27  
28  
29  
30  
31  
32  
33  
34  
35  
36  
37  
38  
39  
40  
41  
42  
43  
44  
45  
46  
47  
48  
49  
50  
51  
52  
53  
54  
55  
56  
57  
58  
59  
60

Fig 1.

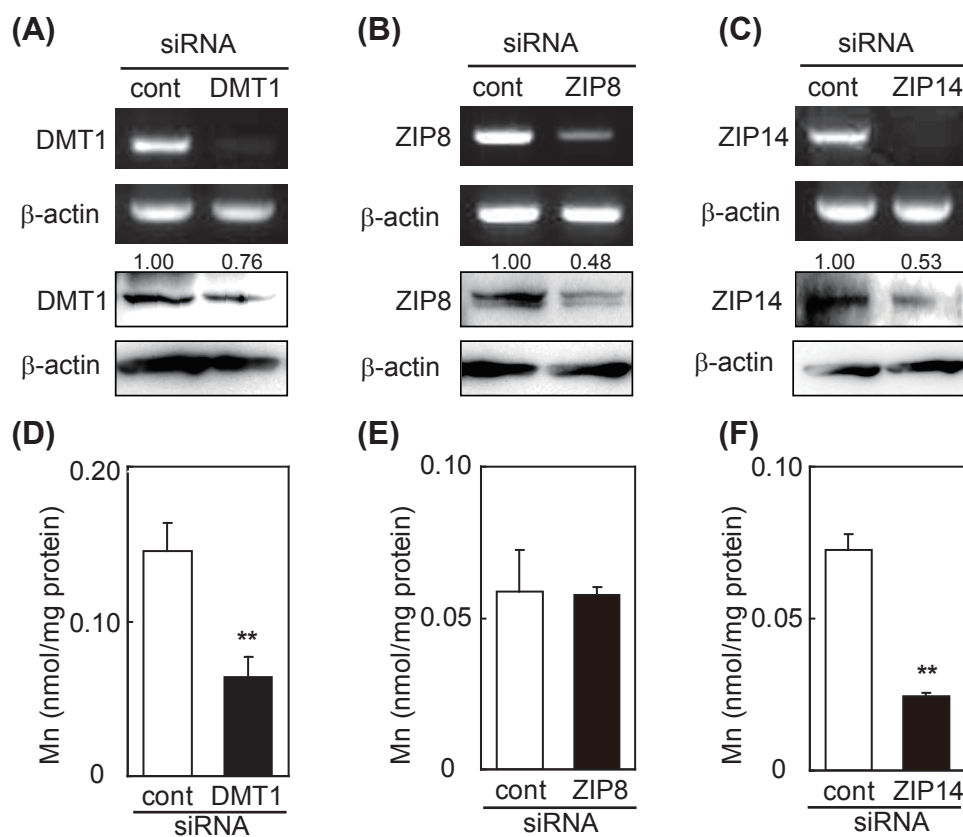
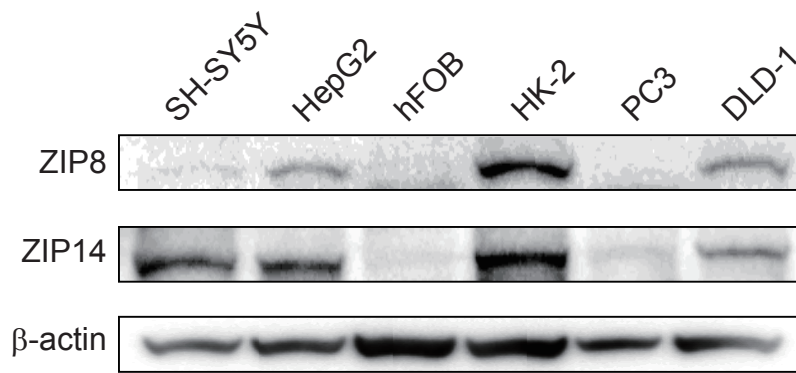


Fig 2.



1  
2  
3  
4  
5  
6  
7  
8  
9  
10  
11  
12  
13  
14  
15  
16  
17  
18  
19  
20  
21  
22  
23  
24  
25  
26  
27  
28  
29  
30  
31  
32  
33  
34  
35  
36  
37  
38  
39  
40  
41  
42  
43  
44  
45  
46  
47  
48  
49  
50  
51  
52  
53  
54  
55  
56  
57  
58  
59  
60

Fig 3.

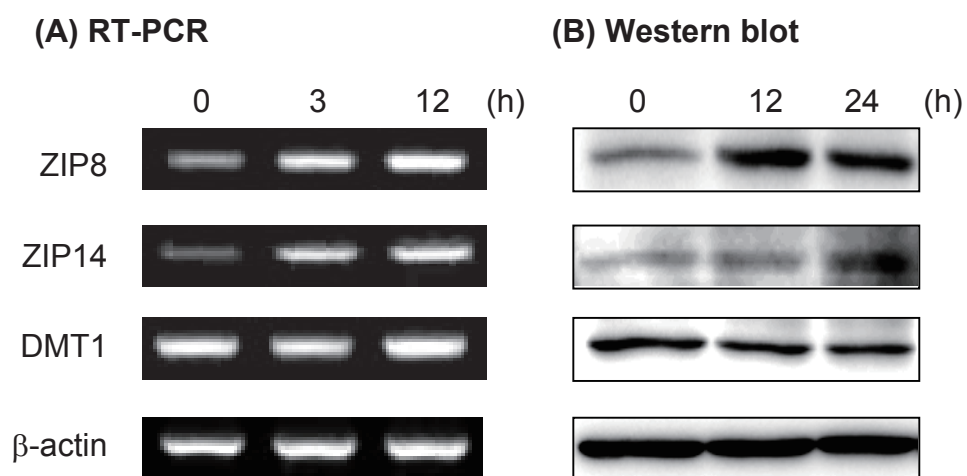
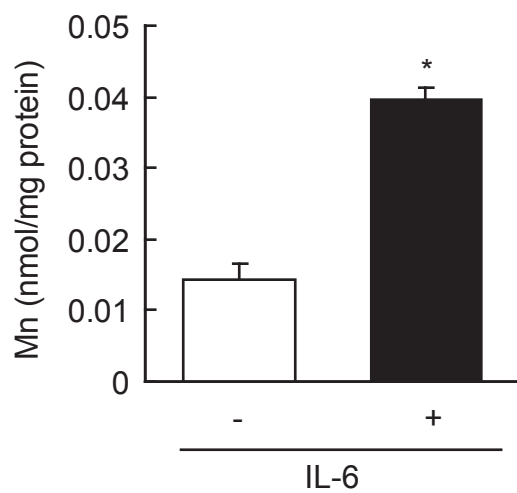


Fig 4.

(A) 24 h-accumulation



(B) 1 h-uptake

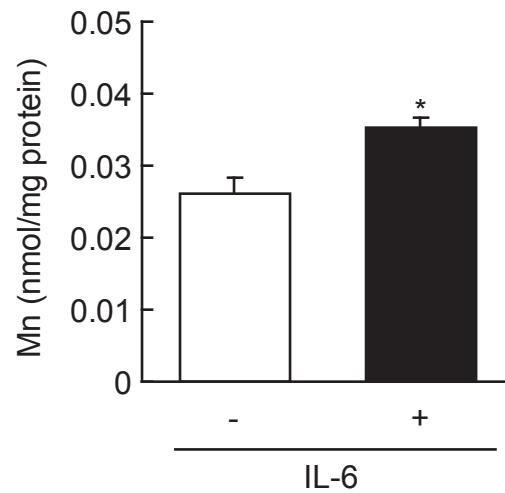
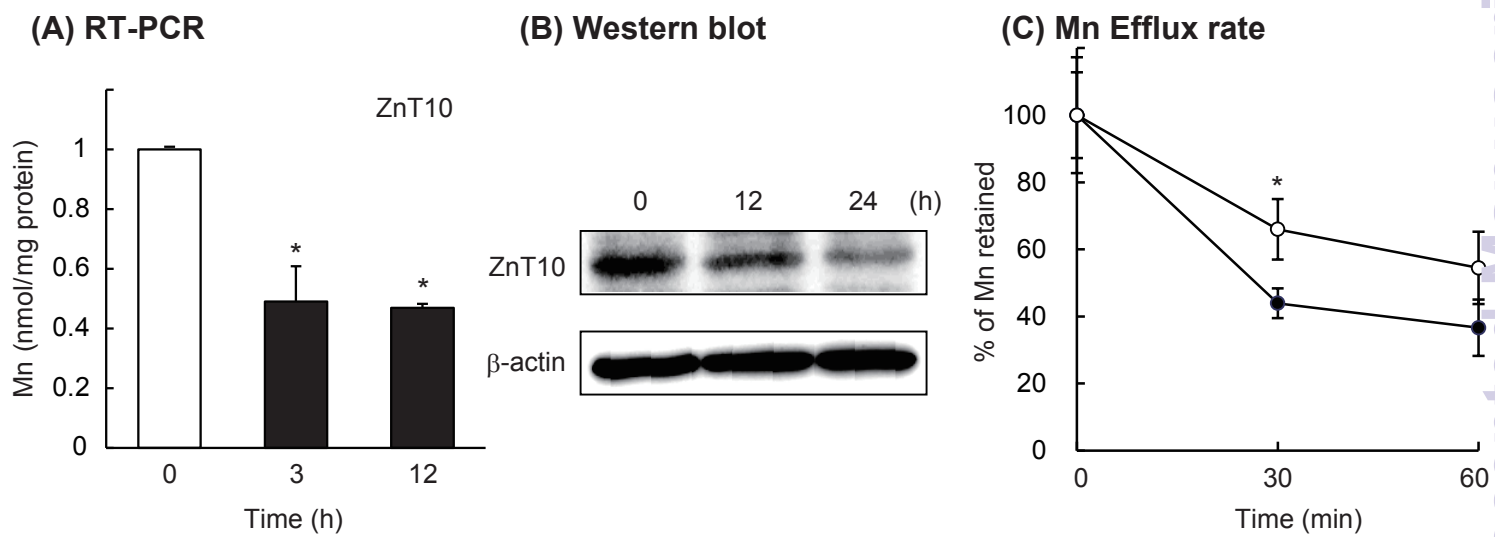


Fig 5.



1  
2  
3  
4  
5  
6  
7  
8  
9  
10  
11  
12  
13  
14  
15  
16  
17  
18  
19  
20  
21  
22  
23  
24  
25  
26  
27  
28  
29  
30  
31  
32  
33  
34  
35  
36  
37  
38  
39  
40  
41  
42  
43  
44  
45  
46  
47  
48  
49  
50  
51  
52  
53  
54  
55  
56  
57  
58  
59  
60